# Residue excitation functions from complete fusion of $^{16}O$ with $^{197}Au$ and $^{208}Pb$

K.-T. Brinkmann, A.L. Caraley, B.J. Fineman, N. Gan, J. Velkovska, and R.L. McGrath
*Physics Department, State University of New York at Stony Brook, Stony Brook, New York 11794*
(Received 31 August 1993)

Evaporation residue excitation functions and $\alpha$-multiplicities from complete fusion of $^{16}O$ with $^{197}Au$ and $^{208}Pb$ have been measured from the fusion threshold up to 140 MeV incident energy. The data allow the conclusion that strongly overdamped motion cannot be dominant at energies in the vicinity of the fusion barrier below $E^* \approx 50$ MeV. At excitation energies above 50 MeV the residue cross section for $^{16}O + ^{208}Pb$ is much greater than predicted from the statistical model with conventional parametrizations. The enhancement is not explained by incorporating dynamical effects into the analysis. An alternative suggestion based on deexcitation-chain dependent fission barriers is discussed.

PACS number(s): 25.70.Gh, 25.70.Jj

## I. INTRODUCTION

Fusion reactions between heavy nuclei can provide important insight into the dynamics and decay properties of excited nuclear matter at moderate excitation energies. Recently, experimental [1] and theoretical [2] attention has focused on $^{16}O + ^{208}Pb$ because this system seems well suited for the study of dynamical effects believed to determine the fission lifetimes of heavy compound nuclei. Both [1] and [2] note that little is known about the cross sections for the formation of evaporation residues (ER's) at high excitation energies and point out that their excitation function may be a sensitive probe for dynamical effects which delay the onset of fission. For example, Butsch *et al.* [1] predict an enhancement of the ER cross section at 140 MeV of about a factor of 20 over the statistical model prediction without dynamics. This prediction is based on the evaluation of a measurement of giant dipole resonance (GDR) $\gamma$ rays in coincidence with fission fragments. Their analysis of the $\gamma$ spectra yields a nuclear friction coefficient of $\gamma = 10$ (corresponding to a reduced friction parameter $\beta = 20\times10^{21}$ s$^{-1}$) implying a long equilibrium lifetime. The authors stress that this value is much larger than any estimate of nuclear viscosity using conventional wall or window formalisms (for a detailed discussion, see [1]). In contrast, a recent study [3] concludes that the measurements of prescission particles, i.e., protons and $\alpha$ particles [4] as well as neutrons [5], are compatible with a value of $\beta = 3\times10^{21}$ s$^{-1}$ beyond the saddle point and only a very short time spent in an equilibrium configuration. This value agrees well with the expectations from the wall formula. It would also imply a smaller cross section for the production of evaporation residues.

Previous measurements [6,7] of the residue cross section in this reaction are limited to energies close to the fusion barrier, corresponding to excitation energies of less than 40 MeV in the compound system $^{224}Th^*$. Furthermore, the two data sets disagree by about a factor of 4 for the peak cross section which remains unexplained. This discrepancy has an important bearing for the interpretation of other measurements because the relative strengths of residue formation and fission at low $E^*$ are routinely used to define the parameters of the statistical model calculations needed to establish the time scales of fission; see, e.g., [8,9].

In view of the uncertain experimental situation we decided to remeasure the excitation function and extend it toward higher excitation energies. In an effort to eliminate as many sources of error as possible the residue production in fusion reactions of $^{16}O$ with $^{197}Au$ was chosen as a calibration standard. It offers the advantages of very similar mass and energy, and has been measured twice [8,10] with virtually the same results. Although leading to an only slightly less fissile compound nucleus, $^{213}Fr^*$, the cross section for ER's is about two orders of magnitude larger than that reported for $^{16}O + ^{208}Pb$ by Vulgaris and co-workers [6].

An additional motivation for the present study are reports that ER cross sections for various neutron-deficient Th and other transactinide compound nuclei formed in more mass-symmetric reactions [11,12] are much enhanced at high excitation energies compared to statistical model predictions. Especially the production of residues associated with $\alpha$ emission is favored. Morawek and coworkers [11] originally suggested that this may be due to the emission of $\alpha$ particles from extended shapes during the formation stage, which is expected to be relatively long for mass-symmetric systems. The present experiment permits the extraction of $\alpha$ multiplicities associated with residues, and investigates these effects in a very asymmetric target-projectile combination.

## II. EXPERIMENT

The experiment was performed at the Stony Brook Linac which delivered $^{16}O$ beams of $\geq 1$ pnA at energies up to 140 MeV. Thin targets (170 $\mu$g/cm$^2$ self-supporting Au and 70 $\mu$g/cm$^2$ isotopically enriched $^{208}Pb$ on a 10 $\mu$g/cm$^2$ carbon backing, respectively) were used.

Evaporation residues were separated from the beam and beamlike reaction products by means of electrostatic deflector plates [13] mounted close to the target ($d = 15$ cm) to allow maximum collection efficiency. The residues were detected in a vertical array of three 400 mm$^2$ surface barrier detectors (SBD's) located 65 cm downstream and displaced by 8 cm in plane with respect to the beam axis. The center-to-center separation between adjacent detectors was 4 cm, corresponding to 3.6°. The SBD's were chosen for their excellent pulse height performance and operability at high field strengths to facilitate the detection of massive ER's with energies of only about 5 MeV. The ER's were separated from the background using their time-of-flight–pulse-height relation. Figure 1 shows a typical spectrum of this kind for $^{16}O + {}^{197}Au$ at 120 MeV incident energy and a deflector voltage of ±10 kV. The ER's are cleanly separated from the background. Also visible are horizontal bands of $\alpha$ particles emitted by residues after they have been implanted in the detector. These interfere with the high-velocity end of the ER spectra at the higher beam energies, but could be readily subtracted by displacing the two-dimensional gates into regions where neither ER's nor a beam-related background are expected. A monitor detector at 28.4° with a defining aperture allowed normalization to Rutherford scattering for all runs.

The efficiency calibration of the whole apparatus was accomplished in an auxiliary experiment where the target recoils from elastic backscattering of 40 MeV $^{16}O$ were detected. Both recoil singles and recoils in coincidence with $^{16}O$ ejectiles emitted at 175° on either side of the beam were recorded, permitting the adjustment of the parameters entering the trajectory calculation [14] which traces ions on their way through the deflector plates. The small angle scattering for these ions, which was treated as the free parameter in the fit to the scattering data, was found to be much larger than predicted by the widely used Meyer prescription [15].

The charge state distributions of detected ions were

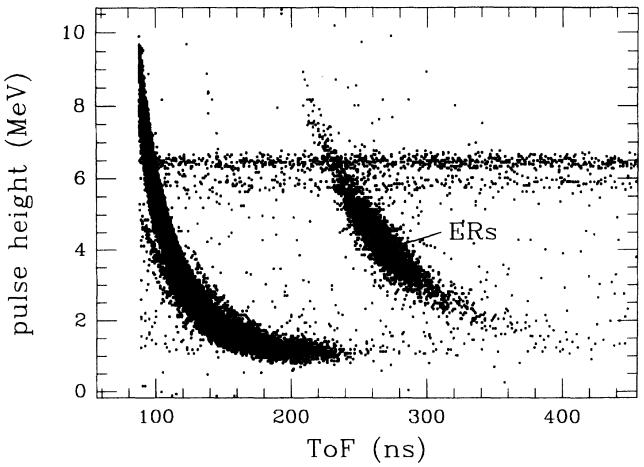


FIG. 1. Typical time of flight (TOF) vs pulse height matrix, for $^{16}O+{}^{197}Au$ at 120 MeV, ±10 kV on the deflector plates. The position of ER's is indicated in the plot.

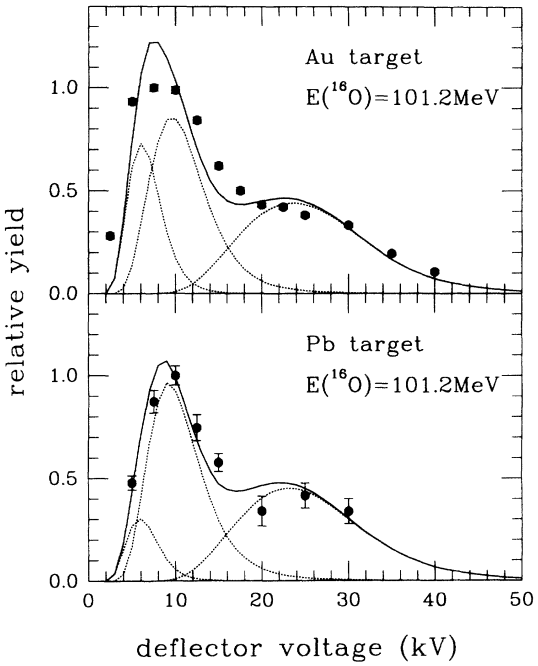


FIG. 2. Voltage distributions of residues at 100 MeV incident energy for both targets. The fits are shown as solid lines; the dotted lines indicate the three components of the charge state distribution.

scanned at principal beam energies of 90, 100, 110, 120, and 134 MeV through the variation of the deflection voltage from 0 to ±40 kV, which covers the range of charge states $q \geq 5$. For the recoils an equilibrium charge state distribution calculated from the formulas summarized in [16] was found appropriate. The residue distributions, however, exhibit a strong component at much higher charge states due to long-lived nuclear states decaying through Auger cascades following inner conversion. The resulting distributions are readily described using the equilibrium distribution and two Gaussians accounting for up to two successive inner conversion cascades as described in [17] and fitting their relative strengths, as shown in Fig. 2. Data for only one voltage setting of ±10 kV were taken at several intermediate energies.

Velocity spectra for each detector, voltage setting, and beam energy were constructed from the projections of the residue gates onto the TOF axis. Where applicable, the spectra were summed over all available voltage settings. The velocity spectra for both targets and incident energies from 89 MeV up to 134 MeV are shown in Fig. 3 for the central detector.

## III. DATA ANALYSIS AND RESULTS

While the input to the efficiency calculations for the recoils is given by simple kinematics, additional information is needed in case of the residues concerning their decay history. In a first approximation, their decay pattern was taken from a Monte Carlo-type statistical model

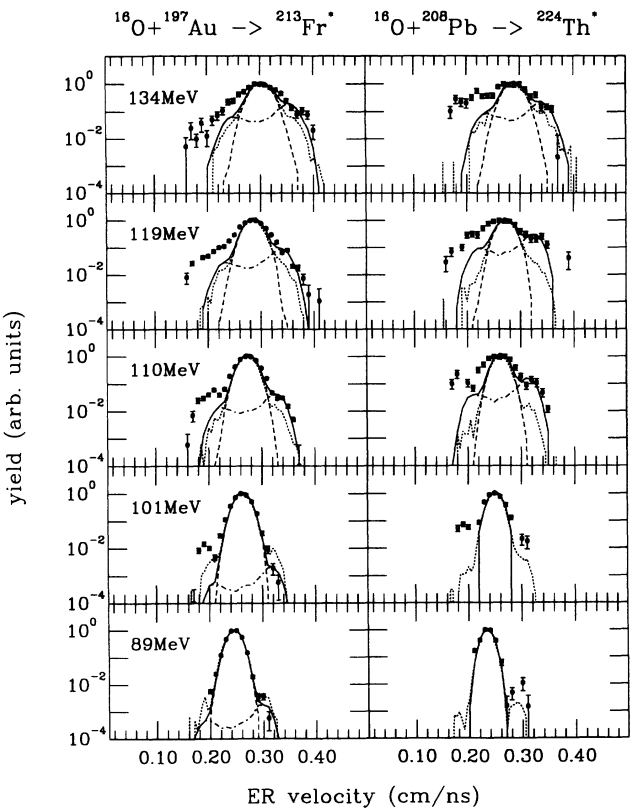


FIG. 3. Velocity distributions of residues at the different beam energies for the Au (left) and Pb target (right) as measured in the central detector. The dotted lines show distributions calculated from a statistical model; the solid lines depict the best fits when ($xnyp$) and ($\alpha xnyp$) mechanisms are treated separately. The latter are also shown as the dashed and dash-dotted lines, respectively.

calculation using a modified version of CASCADE [18,19]. However, this yields a poor description of the measured ER velocity spectra at high incident energies and for velocities substantially higher and lower than the compound nucleus velocity, as shown by the dotted lines in Fig. 3. Processes such as incomplete fusion and preequilibrium emission add to the low-velocity portions of the spectra. Their contribution increases with beam energy. At high velocities, the mismatch is indicative of the failure of the "standard" statistical model calculation to describe the $\alpha$ multiplicities associated with ER's.

In order to account for the shape of the spectra at high velocity, the ($xnyp$) and ($\alpha xnyp$) channels were treated separately in the next set of calculations, leaving their relative strengths as a free parameter which was fitted to the measured velocity spectra. The energy distributions as given by CASCADE were used and the emission was assumed to be isotropic in the center of mass of the emitter. This procedure yields a greatly improved description of the velocity spectra, as shown by the solid lines in Fig. 3. The dashed lines depict the contributions from ($xnyp$) reactions; the dash-dotted lines are for ($\alpha xnyp$) reactions. The peculiar shapes of the latter are due to the kinematic bias of the setup. ER's which emitted $\alpha$ particles backward are detected with the highest efficiency; hence the high-velocity component appears enhanced. The efficiency is greatly reduced for sideways emission of $\alpha$ particles corresponding to velocities close to the compound nucleus (CN) value. Finally, ER's which emitted particles forward are again detected with higher efficiency. (This also implies that our results depend on the angular distribution of evaporated particles, assumed here to be isotropic. The uncertainty related to this assumption is addressed below.) The excess of residues with low velocities over the fit assuming complete fusion, i.e., full momentum transfer, increases with beam energy up to about 25% of the total yield at the highest incident energy. This fraction of the distribution was rejected for the following analysis.

Only the velocity spectra at principal beam energies were deconvoluted. The cross sections at intermediate energies were obtained using interpolated values for the fraction of either mechanism and for the calculated efficiencies. This is justified because neither the velocity spectra nor the charge state distributions exhibit any rapid change as a function of beam energy.

After calculation of the efficiencies for both ($\alpha xnyp$) and ($xnyp$) ER formation mechanisms separately, cross sections were determined by averaging the results from the three detectors. These are displayed in Fig. 4 as a function of excitation energy. Table I summarizes the cross sections for each decay branch, the total cross sec-

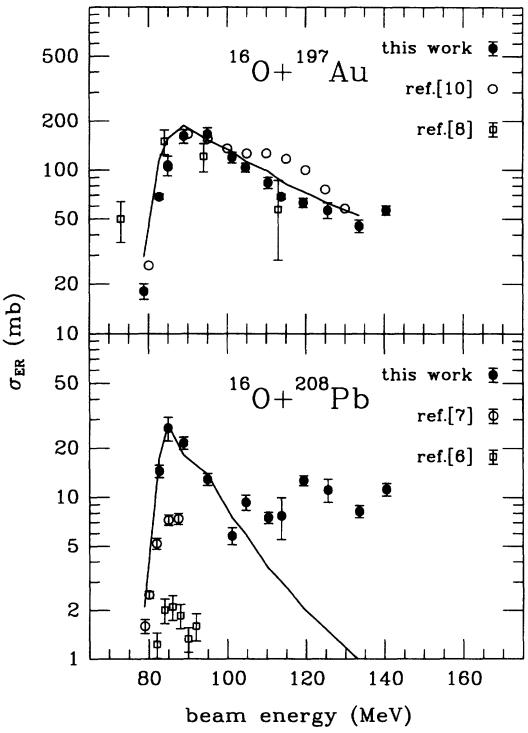


FIG. 4. Absolute cross sections for evaporation residue production in both reactions as a function of beam energy compared to results of other authors; upper frame, $^{16}O+^{197}Au$; solid points, this work; open circles from [10], squares from [8]; lower frame, $^{16}O+^{208}Pb$, solid points, this work; open circles from [6], squares from [7]. The solid lines show statistical model calculations discussed in the text.

TABLE I. Experimental cross sections for $\sigma(xnyp)$, $\sigma(\alpha xnyp)$ channels, and their sum as a function of incident energy $E_{\rm lab}$. Excitation energies $E^*$ are also given. $\alpha$ multiplicities are listed only for energies where the fit to the velocity spectra was performed. The errors are discussed in the text.

| CN | $E_{\rm lab}$ (MeV) | $E^*$ (MeV) | $\sigma(xnyp)$ (mb) | $\sigma(\alpha xnyp)$ (mb) | $\sigma$ (mb) | $\alpha$ |
|---|---|---|---|---|---|---|
| $^{213}$Fr* | 78.8 | 44.2 | 18.1 | 0 | 18.1 ± 2.0 | |
| | 82.7 | 47.8 | 68.5 | 0 | 68.5 ± 6.9 | |
| | 84.9 | 49.8 | 106.9 | 0 | 106.9 ± 15 | |
| | 88.9 | 53.5 | 161.1 | 0 | 161.1 ± 16 | 0.00 ± 0.05 |
| | 94.9 | 59.0 | 165.8 | 0 | 165.8 ± 17 | |
| | 101.2 | 64.9 | 119.1 | 0 | 119.1 ± 8.9 | 0.00 ± 0.05 |
| | 104.7 | 68.1 | 91.1 ± 9.1 | 12.3 ± 1.2 | 103.4 ± 9.2 | |
| | 110.4 | 73.4 | 62.3 ± 6.2 | 21.1 ± 2.4 | 83.4 ± 6.6 | 0.25 ± 0.03 |
| | 113.8 | 76.5 | 45.0 ± 4.5 | 23.5 ± 2.4 | 68.5 ± 5.1 | |
| | 119.4 | 81.7 | 37.6 ± 3.0 | 25.4 ± 2.8 | 63.0 ± 4.0 | 0.40 ± 0.05 |
| | 125.6 | 87.4 | 26.7 ± 2.7 | 26.7 ± 4.8 | 56.6 ± 5.5 | |
| | 133.6 | 94.8 | 17.9 ± 1.5 | 27.3 ± 3.7 | 45.2 ± 4.0 | 0.60 ± 0.10 |
| | 140.5 | 101.2 | 12.5 ± 0.9 | 44.1 ± 3.5 | 56.6 ± 3.6 | 0.78 ± 0.08 |
| $^{224}$Th* | 78.8 | 29.2 | 0.4 ± 0.2 | 0 | 0.4 ± 0.2 | |
| | 82.7 | 32.9 | 14.5 | 0 | 14.5 ± 1.5 | |
| | 84.9 | 34.9 | 26.6 | 0 | 26.6 ± 4.4 | |
| | 88.9 | 38.6 | 21.6 | 0 | 21.6 ± 1.9 | 0.00 ± 0.06 |
| | 94.9 | 44.2 | 12.9 | 0 | 12.9 ± 1.3 | |
| | 101.2 | 50.0 | 5.8 | 0 | 5.8 ± 0.7 | 0.00 ± 0.06 |
| | 104.7 | 53.3 | 6.9 ± 0.8 | 2.4 ± 0.6 | 9.3 ± 1.0 | |
| | 110.4 | 58.6 | 4.6 ± 0.4 | 3.0 ± 0.4 | 7.5 ± 0.6 | 0.39 ± 0.06 |
| | 113.8 | 61.7 | 3.2 ± 1.2 | 4.5 ± 1.9 | 7.7 ± 2.2 | |
| | 119.4 | 66.9 | 3.8 ± 0.3 | 8.9 ± 0.8 | 12.7 ± 0.9 | 0.70 ± 0.08 |
| | 125.6 | 72.7 | 3.2 ± 0.6 | 7.9 ± 1.7 | 11.1 ± 1.8 | |
| | 133.6 | 80.1 | 3.3 ± 0.4 | 4.9 ± 0.5 | 8.2 ± 0.7 | 0.60 ± 0.08 |
| | 140.5 | 86.5 | 2.2 ± 0.2 | 9.0 ± 0.9 | 11.2 ± 1.0 | 0.80 ± 0.11 |

tions, and $\alpha$ multiplicities. The figure also contains results for energies where only one voltage setting was studied, as described above.

Cross sections determined for individual detectors deviated from the average by less than 10% in all cases where the full voltage distribution was studied, and we regard this as an indication of the reliability in extracting relative cross sections. For these cases the uncertainties were taken as the standard deviation of the average over all voltages and detectors. For energies where only one voltage was measured an error of ±10% for the separate $(xnyp)$ and $(\alpha xnyp)$ channels was adopted unless deviations between detectors or statistical uncertainties turned out to be larger. Especially at low energies where the $(xnyp)$ channel dominates, the ER yield varies considerably with angle (detector), i.e., by up to a factor of 2 in going from 0° to 3.6°. For these data it is evident that our efficiency calculations account for the observed distributions.

However, for the $(\alpha xnyp)$ channels the angular distribution widths are larger than the detector separation so that the data cannot confirm the validity of the efficiency calculations. We have explored the effect of changing the assumption that alphas are evaporated isotropically. Following the semiclassical description of [20], the anisotropy of alphas may be as large as $W(0°)/W(90°) \approx 1.3$, which would reduce the $(\alpha xnyp)$ cross sections reported here by less than 10%. With such considerations and taking into account uncertainties in detector and deflector positioning, we conclude that the cross section measurements have an overall systematic error of less than 20%.

Along with the cross sections, $\alpha$ multiplicities were deduced which are shown in Fig. 5. They are based on the assumption that not more than one $\alpha$ particle per

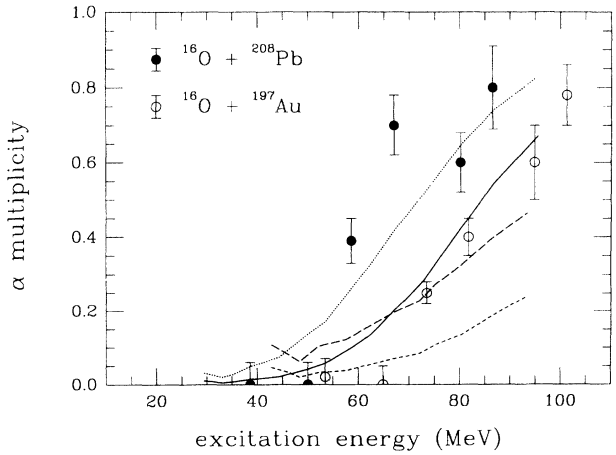


FIG. 5. $\alpha$ multiplicities associated with evaporation residues (open symbols, $^{16}$O+$^{197}$Au; solid points, $^{16}$O+$^{208}$Pb). Calculations with standard parameters (short-dashed and solid lines, respectively) and using optical model radii increased by 10% (long-dashed and dotted lines, respectively) are also shown.

compound nucleus was emitted, which is verified by the overall agreement of calculated and measured velocity spectra.

The evaporation excitation functions reported by Baba *et al.* [10] and Hinde *et al.* [8] for $^{213}$Fr* and by Vulgaris *et al.* [6] and Hartel [7] for $^{224}$Th* are included in Fig. 4 as well as calculations which will be discussed later. For the $^{213}$Fr* compound system all three experiments show reasonable agreement in overall shape and magnitude. There are some differences in detail. For example, the results of [8] are shifted towards lower energy by about 5 MeV, while our data agree with [10]. Also, at higher excitation energy, the excitation function of [10], which identified residues by their characteristic $\alpha$ and $\gamma$ decays, exhibits some structure which is not reproduced here. For $^{224}$Th*, the three available data sets do not agree at all. The reason for this discrepancy is not clear. Since our data have been obtained with a reference standard measured simultaneously, we believe that the present results are accurate.

Comparing the new results for both systems, the cross sections not only differ by about an order of magnitude, but the excitation functions also exhibit a qualitative shape difference. While the cross section for ER's from $^{213}$Fr* decreases with energy above 100 MeV, the data for $^{224}$Th* show a constant value of $\approx$ 10 mb. The $\alpha$ multiplicities associated with $^{224}$Th*-ER's increase at a much steeper rate and at lower excitation energy than those for $^{213}$Fr*. Possible explanations for these differences will be evaluated in the following section.

## IV. DISCUSSION

The experimental data were compared to calculations performed with the statistical model code CASCADE [18,19]. Whenever appropriate, e.g., when dynamical effects were included in the calculation, a modified Monte Carlo version (see, e.g., [14]) was used. The calculations are displayed as lines in Figs. 3–7. The fluctuations in these curves are due to the discrete energy steps and the Monte Carlo nature of some of the calculations.

In a first set of calculations the principal statistical model parameters were varied in order to find the parameter set that reproduces the low-energy cross section. As has been noted in the literature (see, e.g., [9,21]), various parameters of the statistical model may be varied in order to describe experimental data. The principal three parameters are the height of the fission barrier, commonly expressed through a scaling factor $k_f$ to the Sierk barriers [22]; the ratio of level density parameters between saddle point and equilibrium shapes, $a_f/a_n$; the level density parameter at equilibrium, $a_n$, itself.

Each of these three parameters was varied independently, keeping the two others at their nominal values, i.e., $k_f$=1, $a_f/a_n$ = 1, and $a_n$=$A$/(9 MeV), respectively. The latter is close to the value found to give the best description of the prefission $\gamma$ spectrum [23] of $^{224}$Th*. Some theoretical guidance for the ratio of level densities is provided in [24], where a shape-dependent level density parameter is calculated. The ratio turns out to be a few percent larger than 1, depending on the compactness of the saddle point configuration of the system under study. All attempts in the literature to determine the ratio $a_f/a_n$ experimentally are consistent with a value of 1. Standard optical model transmission coefficients for neutrons, protons, and $\alpha$ particles [25–27] were used. The fusion cross sections needed for the calculations were obtained as the sum of the ER cross sections and fission cross sections found in the literature. For $^{16}$O+$^{197}$Au the results of [28] were adopted; for $^{16}$O+$^{208}$Pb several measurements exist [6,29,30], which show excellent agreement and were averaged.

None of the three principal parameters has a significant influence on the shape of the calculated excitation function. Table II lists the three parameter sets which describe the excitation function up to about 100 MeV and indicates the sensitivity of the calculation to the parameters. The solid line in Fig. 4 shows a comparison between the data and the calculation in which the factor to the fission barrier was treated as the free parameter. This approach is adopted in the remainder of the discussion, since the close similarity of the two systems makes it unlikely that significant differences in $a_n$ or $a_f/a_n$ exist.

Using a factor of 1.05 to the barrier, the measured ER excitation function for $^{213}$Fr* is remarkably well reproduced by the calculation. For $^{224}$Th* the peak at low energy is described well with $k_f$=0.90. A very small factor of 0.6 was used in the GDR $\gamma$-ray study [1] in accommodating the results previously reported by Vulgaris *et al.* [6]. This is much smaller than one expects on the basis of fission and evaporation cross section studies of various lighter systems (see, e.g., [8] and references therein).[1] At higher energies the calculated $^{224}$Th* excitation function decreases rapidly and severely underpredicts the data which saturate at $\approx$ 10 mb above $E^* \approx$ 50 MeV.

Next, the influence of various formulations of transient delay and viscosity on the model predictions was explored. The results are summarized in Fig. 6. The solid lines correspond to the standard CASCADE calcu-

TABLE II. Statistical model parameter sets yielding a satisfying reproduction of the measured ER excitation functions below 100 MeV. The fitted variable is denoted by the *; the fractions quoted in brackets are the modifications of the standard parameter value required to change the calculated cross section by about 50%.

| CN | $k_f$ | $a_f/a_n$ | $A/a_n$ (MeV) |
|---|---|---|---|
| $^{213}$Fr* | 1.05* (10%) | 1 | 9 |
| | 1 | 0.98* (4%) | 9 |
| | 1 | 1 | 10.0* (20%) |
| $^{224}$Th* | 0.90* (10%) | 1 | 9 |
| | 1 | 1.02* (2%) | 9 |
| | 1 | 1 | 7.4* (20%) |

[1]The authors of Ref. [8] used the rotating liquid-drop model [31] which yields barriers which are about 10 – 20 % higher than Sierk's [22] and find $k_f$ between 0.83 and 1.05.

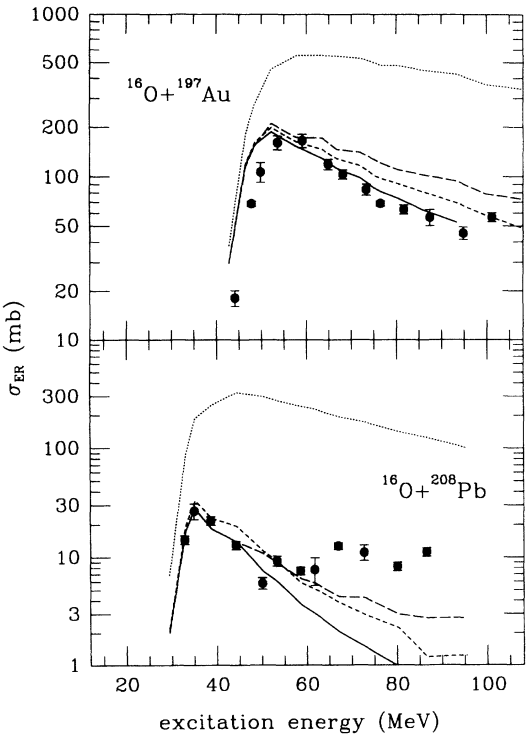


FIG. 6. Statistical model calculations compared to the excitation functions; solid line, best fit to the excitation functions using CASCADE statistical model calculations with the fission barrier height as the only adjustable parameter; dotted line, viscosity as given in [1]; short-dashed line, transient time only; long-dashed line, fission turned off above 50 MeV. See text for details.

lation using the parameters described above, while the dotted lines give the predictions as in [1], using a transient time of $\tau_d = 30\times10^{-21}$ s and $\gamma = 10$ which overpredict both excitation functions severely. In order to reproduce the peak cross sections of the excitation functions, an unreasonable reduction of the fission barriers to 60% for $^{213}$Fr* and 35% for $^{224}$Th* would be required. As discussed above, these values are not compatible with fission barrier systematics. Thus, fission is not overdamped at low excitation energy.

The agreement between experiment and calculation for $^{213}$Fr* appears to be worsened when any transient time spent in an equilibrium configuration is included. For illustration, the short-dashed line shows the effect of a transient time of $\tau_d = 30\times10^{-21}$ s alone. However, it must be noted that too little is known about the energy dependence of any of the parameters entering the statistical model calculation to draw any unambiguous conclusion. For example, Newton *et al.* [32] have pointed out the importance of the temperature dependence of the fission barrier for statistical model calculations. According to their description, the fission barriers are reduced significantly over the temperature range from 1 to 2 MeV. This might yield a residue excitation function decreasing more rapidly with increasing energy, making room for a cross section enhancement due to dynamical effects. So it would be unwarranted to conclude that the data rule out the existence of viscosity and transient time scales at high $E^*$.

No introduction of fission dynamics can describe the ER cross section behavior in $^{224}$Th*. As an example, a calculation assuming a vanishing fission probability above 50 MeV excitation energy, the value where the $^{224}$Th* data and the standard calculation start to deviate, is shown by the long-dashed line in Fig. 6. Even in this extreme case, using the strongest "fission hindrance" still compatible with the data at low excitation energies, the calculation cannot reproduce the enhancement of the cross section for $^{224}$Th*. (We note, however, that the energy at which the deviations occur roughly coincides with the onset of deviations between statistical model predictions and the observed prescission neutron multiplicities [33].)

Not only do the standard calculations fail to reproduce the cross section for $^{224}$Th* above 50 MeV excitation energy, they also drastically underpredict the $\alpha$ multiplicities for both systems, as shown in Fig. 5. The multiplicities are better reproduced if transmission coefficients are used which are calculated assuming an increase in the optical model radius of 10%. This is shown by the long-dashed and dotted lines. A number of authors [34] have reported that the particle emission barriers for $\alpha$ particles have to be reduced in order to describe multiplicities and spectral shapes, suggestive of emitter deformation. Averaging over emission directions [35] for a deformed Th nucleus with a long-to-short axis ratio of 1.5 : 1 gives about the same multiplicity enhancement as a 10% radius increase. A deformation of this magnitude for the average emitter shape is reasonable, since it lies well inside the saddle-point deformation of $\geq 2$ : 1 [31] for partial waves contributing to ER production. Using an optical model radius increased by 10%, the multiplicities associated with residues from the decay of $^{213}$Fr* are well described, but an excess of $\alpha$ particles for $^{224}$Th* at intermediate energies remains. This calculation is shown by the long-dashed and dotted lines in Fig. 5.

Insight into the qualitative difference between the model predictions and experimental data for the excitation functions of $^{224}$Th* compared to $^{213}$Fr* is suggested by low-energy neutron induced fission data. There, the fission barrier heights for Ra isotopes have been measured to be about 8.5 MeV [36], while the Sierk prescription yields values of only about 6.9 MeV at zero angular momentum. For Th, the outer, higher barrier is experimentally determined to be about 6.5 MeV [37], much closer to the Sierk value of 6.3 MeV. Hence, the survival probability of compound nuclei after emission of $\alpha$ particles may actually be higher than predicted by the transition state model with Sierk barriers. It has also been observed in the past [38,39] that fission barriers and/or neutron binding energies deduced on a liquid-drop basis, which are fit to experimental information in the $(Z, A)$ range of interest here, vary in a systematic fashion within isotopic chains and show deviations of several MeV presumably due to shell effects. Thus, allowing substantial variations of the fission barrier heights in a narrow mass

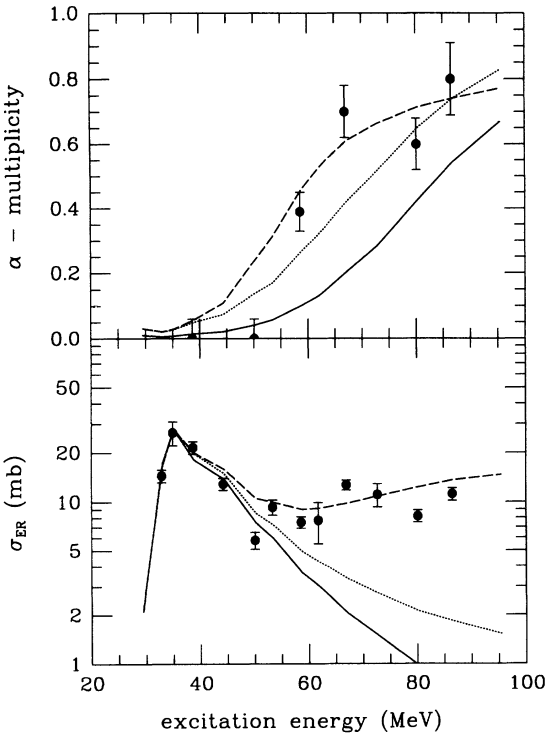


FIG. 7. Cross sections and $\alpha$ multiplicities for $^{16}O + ^{208}Pb$ compared to the standard calculation (solid line), a calculation using optical model radii increased by a factor 1.1 (dotted line), and the latter with an additional modification of fission barrier heights for daughters with $Z$ smaller than $Z_{CN}$ (dashed line).

range is not unreasonable. As an illustrative example, the fission barriers of all daughter nuclei produced through charge emission were scaled by a factor of 1.3, while for Th isotopes the factor 0.9 was kept. This *ad hoc* recipe describes the excitation function and the $\alpha$ multiplicities for residues from $^{16}O + ^{208}Pb$ reactions surprisingly well, as shown in Fig. 7.

Enhanced ER cross sections and $\alpha$ multiplicities in excess of the statistical model predictions have recently also been observed in other transactinide nuclei formed in more symmetric collisions of $^{110}Pd$ with $^{110}Pd$, $^{104}Ru$ [11] as well as of $^{40}Ar$ with several targets yielding compound nuclei of $Z$=90–93 [12]. Morawek *et al.* [11] attribute this effect to the long formation time scale for nearly symmetric systems, which allows emission of charged particles already during the formation stage before the shape degree of freedom equilibrates. Formation times of the order of the first stage lifetime of the CN, $\geq 10^{-20}$ s, were estimated using [40] for the symmetric reactions. In the very asymmetric system $^{16}O+^{208}Pb$ the time the composite system needs in order to evolve toward an equilibrium shape is certainly too short to permit emission of sufficient numbers of $\alpha$ particles ($\approx 2\times10^{-21}$ s according to [40]). Thus, the large $\alpha$ multiplicity observed here buttresses the conjecture that $(Z, A)$ specifics of fission barriers can influence the ER production significantly.

## V. CONCLUSIONS

The cross sections for evaporation residue production in complete fusion reactions of $^{16}O$ projectiles with $^{197}Au$ and $^{208}Pb$ have been studied over a wide energy range. The results for the lighter target are in good agreement with earlier studies [8,10]. The excitation function is well reproduced by statistical model calculations when the fission barrier of Sierk [22] is increased by a factor of 1.05. The $\alpha$ multiplicities are about a factor of 2 larger than predicted by the statistical model using standard optical model parameters. The discrepancy can be reduced using an optical model radius increase of 10% for the calculation of transmission coefficients.

For the heavier system the experiment yields a much larger cross section in the vicinity of the interaction barrier than previously reported by [6] and [7]. The cross section for ER production at low excitation energies is consistent with a factor of 0.90 to the Sierk barriers. The excitation functions for both systems imply that the fission degree of freedom is not overdamped at low temperatures of $\approx$ 1 MeV.

At higher excitation energies the cross sections and $\alpha$ multiplicities for $^{224}Th^*$ exhibit a behavior which is not described by the statistical model using conventional parameter choices. With such choices the cross section saturation cannot be reproduced even by imposing extreme fission hindrance, i.e., setting the fission width to zero for $E^*$ greater than about 50 MeV. Other effects must be responsible, obscuring information about fission dynamics.

The findings in Th at high $E^*$ are similar to those in more symmetric reactions leading to compound nuclei in the transactinide region, which had been interpreted as due to long formation times. This interpretation is not appropriate in the present case since only very short formation times are expected in this very asymmetric reaction. One way to account for the experimental results is by treating the different decay chains with slightly different fission barriers which lie well within the acceptable range of currently available experimental information.

## ACKNOWLEDGMENTS

The authors would like to express their gratitude to the staff at the Nuclear Structure Laboratory in Stony Brook for their continuous support in running the accelerator. The targets were skillfully prepared by A. Lipski. Fruitful discussions with J. Alexander, P. Paul, B.B. Back, and D.J. Hofman are gratefully acknowledged. This work was sponsored in part by the U.S. National Science Foundation.

[1] R. Butsch, D.J. Hofman, C.P. Montoya, P. Paul, and M. Thoennessen, Phys. Rev. C **44**, 1515 (1991).
[2] P. Fröbrich and I.I. Gontschar, Nucl. Phys. **A563**, 326 (1993).
[3] J.P. Lestone, in Ninth Winter Workshop on Nuclear Dynamics, Key West, 1993 (unpublished); Phys. Rev. Lett. **70**, 2245 (1993).
[4] J.P. Lestone, J.R. Leigh, J.O. Newton, D.J. Hinde, J.X. Wei, J.X. Chen, S. Elfstrom, and D.G. Popescu, Phys. Rev. Lett. **67**, 1078 (1991).
[5] D.J. Hinde, D. Hilscher, H. Rossner, B. Gebauer, M. Lehmann, and M. Wilpert, Phys. Rev. C **45**, 1229 (1992).
[6] E. Vulgaris, L. Grodzins, S.G. Steadman, and R. Ledoux, Phys. Rev. C **33**, 2017 (1986).
[7] K. Hartel, Ph.D. thesis, Technical University, Munich, 1985.
[8] D.J. Hinde, R.J. Charity, G.S. Foote, J.R. Leigh, J.O. Newton, S. Ogaza, and A. Chatterjee, Nucl. Phys. **A452**, 550 (1986).
[9] R.J. Charity, J.R. Leigh, J.J.M. Bokhorst, A. Chatterjee, G.S. Foote, D.J. Hinde, J.O. Newton, S. Ogaza, and D. Ward, Nucl. Phys. **A457**, 441 (1986).
[10] S. Baba, K. Hata, S. Ichikawa, T. Sekine, Y. Nagame, A. Yokoyama, M. Shoji, T. Saito, N. Takahashi, H. Baba, and I. Fujiwara, Z. Phys. A **331**, 53 (1988).
[11] W. Morawek, D. Ackermann, T. Brohm, H.-G. Clerk, U. Gollerthan, E. Hanelt, M. Horz, W. Schwab, B. Voss, K.-H. Schmitt, and F.P. Hessberger, Z. Phys. A **341**, 75 (1991).
[12] F.P. Hessberger, V. Ninov, and D. Ackermann, Z. Phys. A **343**, 301 (1992).
[13] R. Schicker, N. Alamanos, P. Braun-Munzinger, J. Stachel, and L. Waters, Nucl. Instrum. Methods A **269**, 585 (1988).
[14] B.J. Fineman, K.-T. Brinkmann, A.L. Caraley, N. Gan, W.J. Kernan, and R.L. McGrath, The Nuclear Structure Laboratory Progress Report 1990–1992, Stony Brook, 1992, p. 96ff.
[15] L. Meyer, Phys. Status Solidi B **44**, 253 (1971).
[16] B. Delauny, Nucl. Instrum. Methods **146**, 101 (1977).
[17] V. Metag, D. Habs, H.-J. Specht, G. Ulfert, and C. Kozhuharov, Hyperfine Inter. **1**, 405 (1976); G. Ulfert, D. Habs, V. Metag, and H.J. Specht, Nucl. Instrum. Methods **148**, 369 (1978).
[18] F. Pühlhofer, Nucl. Phys. **A280**, 267 (1977).
[19] M. Herman, University of Rochester Nuclear Structure Laboratory Report No. UR-NSRL-318, 1987 (unpublished).
[20] L.C. Vaz, J.M. Alexander, and N. Carjan, Z. Phys. A **324**, 331 (1986).
[21] J.O. Newton, D.J. Hinde, R.J. Charity, J.R. Leigh, J.J.M. Bokhorst, A. Chatterjee, G.S. Foote, and S. Ogaza, Nucl. Phys. **A483**, 126 (1988).
[22] A.J. Sierk, Phys. Rev. C **33**, 2039 (1986).
[23] M. Thoennessen, D.R. Chakrabarty, M.G. Herman, R. Butsch, and P. Paul, Phys. Rev. Lett. **59**, 2860 (1987).
[24] J. Tõke and A.J. Swiatecki, Nucl. Phys. **A372**, 141 (1981).
[25] D. Wilmore and P.E. Hodson, Nucl. Phys. **55**, 673 (1964).
[26] F.G. Perey, Phys. Rev. **131**, 745 (1963).
[27] L. McFadden and G.R. Satchler, Nucl. Phys. **84**, 177 (1966).
[28] T. Sikkeland, Phys. Rev. **135**, B669 (1964).
[29] B.B. Back, R.R. Betts, J.E. Gindler, B.D. Wilkins, S. Saini, M.B. Tsang, C.K. Gelbke, W.G. Lynch, M.A. McMahan, and P.A. Baisden, Phys. Rev. C **32**, 195 (1985).
[30] F. Videbæck, R.B. Goldstein, L. Grodzins, S.G. Steadman, T.A. Belote, and J.D. Garrett, Phys. Rev. C **15**, 954 (1977).
[31] S. Cohen, F. Plasil, and W.J. Swiatecki, Ann. Phys. (N.Y.) **82**, 557 (1974).
[32] J.O. Newton, D.G. Popescu, and J.R. Leigh, Phys. Rev. C **42**, 1772 (1990).
[33] D. J. Hinde, D. Hilscher, and H. Rossner, Nucl. Phys. **A502**, 497c (1989).
[34] See, e.g., W.E. Parker, M. Kaplan, D.J. Moses, G. La Rana, D. Logan, R. Lacey, J.M. Alexander, D.M. de Castro Rizzo, P. DeYoung, R.J. Welberry, and J.T. Boger, Phys. Rev. C **44**, 774 (1991); H. Ikezoe, N. Shikazono, Y. Nagame, Y. Sugiyama, Y. Tomita, K. Ideno, A. Iwamoto, and T. Ohtsuki, *ibid.* **42**, R1187 (1990).
[35] J.R. Huizenga, A.N. Behkami, I.M. Govil, W.U. Schröder, and J. Tõke, Phys. Rev. C **40**, 668 (1989).
[36] H. Groening and W. Loveland, in *Proceedings of the International Conference on Physics and Chemistry of Fission, Rochester, 1973* (IAEA, Vienna, 1974), Vol. I, p. 39.
[37] B.B. Back, O. Hansen, H.C. Britt, J.D. Garrett, and B. Leroux, in *Proceedings of the International Conference on Physics and Chemistry of Fission* [36], Vol. I, p. 3; B.B. Back, O. Hansen, H.C. Britt, and J.D. Garrett, in *ibid.*, Vol. I, p. 25.
[38] K.-H. Schmitt, W. Faust, G. Münzenberg, W. Reisdorf, H.-G. Clerc, D. Vermeulen, and W. Lang, in *Proceedings of the International Conference on Physics and Chemistry of Fission*, Jülich, 1979 (IAEA, Vienna, 1980), Vol. I, p. 409.
[39] D. Vermeulen, H.-G. Clerc, C.-C. Sahm, K.-H. Schmitt, G. Münzenberg, and W. Reisdorf, Z. Phys. A **318**, 157 (1984).
[40] H. Feldmeier, in *Nuclear Structure and Heavy Ion Dynamics*, edited by L. Moretto and R.A. Ricci (North-Holland, Amsterdam, 1984), p. 274.